Electronic Supplementary Material (ESI) for Analyst.

Supporting Information

Related to

Discrete Fast Fourier Transform-Assisted Ultraviolet-Infrared Dual Resonance Spectroscopy for Aerosol Detection and Identification

Marjan Rejaei Ramsheh, Mohammad Mahdi Doroodmand*

Department of Chemistry, College of Sciences, Shiraz University, Shiraz 71454, Iran.

***Corresponding Author**: Doroodmand@shirazu.ac.ir, Doroodmand@yahoo.com, Tel: +098-713-6137152, Fax: +098-713-6460788.

Contents

1.SI. Introduction

1.1.SI. Importance of aerosols

1.2.SI. Aerosols analysis

1.3.SI. Double resonance spectroscopy

2.SI. Experimental

2.1.SI. Sample Introduction system

2.2.SI. Calibration of the aerosol-based detection system

2.3.SI. Estimation of the fingerprint frequencies

3.SI. Results and discussion

3.1.SI. Reliability of the detection system

3.1.1.SI. Plasmatic resonance of Ag nanoparticles

3.1.2.SI. Middle infrared analysis of polycarbonate powders

3.2.SI. Synergistic effects of ultraviolet-infrared dual radiations

3.3.SI. Fourier transform-assisted ultraviolet-infrared dual resonance spectroscopy

3.4.SI. FID averaging based on the switching property of the UV radiation

3.5.SI. Dual resonance between UV and far/near IR

3.6.SI. Figures of merit

3.6.1.SI. Qualitative analysis: Type of Aerosols

3.6.2.SI. Quantitative aspect of the detection system for particle counting purposes

3.7.SI. Real sample analysis

3.8. Comparison

References

1.SI. Introduction

1.1.SI. Importance of aerosols

Strictly speaking the term aerosol includes both the particles and the suspending gas [1,2]. Usually discuss aerosols as "*Desirable*" or "*Undesirable*". The first one includes special cases, produced specifically for their beneficial properties (e.g. nanotechnology, ceramic powders). Whereas, the latter is often associated with the use of potentially harmful to human health (for example, spectacular) [3]. Particulate matter is at the core of environmental problems such as global warming, photochemical smog, stratospheric ozone, and poor air quality [3,4, 1,5].

The aerosol's particle size range often varies from a few nanometers to a few tens of microns [6]. Bio-aerosol is including viruses, bacteria cells and spores, fungi, pollen, as well as their constituents and components, their aggregates and fragments [7,8]. Biological warfare is also known as "*Germ Warfare*". The use of biological toxins or infectious agents such as bacteria, viruses and fungi to kill or disable humans, animals or plants as an act of warfare [9,10]. An aerosol attacks with biological agents would work optimally as a fine mist of 1–5 μm particle size [11]. All of the above information points to the high demand and the need to determine the extent of chemical/biochemical modified aerosols such as fog, dust, water droplets, etc. [12,13].

However, intrinsic behavior of the aerosols especially their small diameter, random motion, multiple particles, their high active surface area, and the electrical charge of the aerosols, majorly limits the aerosols detection systems to the "*Optical Spectroscopy*", based on different optical properties of the aerosols [13,14]. At this conditions, obviously, besides factors such as selectivity, sensitivity, fast analysis time, improved detection limits, "*Real-Time Sample Analysis*" is considered as very important parameter related to the figures of merit for the aerosol detection purposes [14].

1.2.SI. Aerosols analysis

Analysis of aerosol particles may involve a wide range of applications and technical disciplines and employ a variety of experimental techniques [15,16]. Consequently, characterization of these aerosol populations often are focused on different techniques such as particle size distributions, particle number densities, total species concentrations, and particle species composition [16,17]. There are a number of measurement techniques available that provide different particle parameters; however, it is important to consider the characteristics of the particular aerosol system of interest, when selecting a suitable measurement technique [17,18]. Techniques adopted the physical properties of aerosol particle populations contain the analysis of the mobility and scattering of often Mie light scattering [19]. This spectroscopic property can provide integrated measurement of parameters such as total number density or mass concentration or measurement of aerosol size distribution classification using off-line methods[19,20].

However, some spectroscopic parameters for aerosol and bio-aerosol detection and recognition such as fluorescence spectroscopy, atomic emission spectroscopy, flame emission spectroscopy, laser induced breakdown spectroscopy, “Mass Spectrometry”, Raman spectroscopy and terahertz spectroscopy have been reported [18–21]. These methods have some disadvantages such as low specificity, small sensitivity of the detection system, high cost and not-real time analysis that often limited their applications [21]. This is due to the significant challenges in current technologies of existing airborne particle-based systems such as insufficient selection, low recovery detection limitations, real-time analysis, unavailability, high cost, portability, Long analysis time, etc. Thus, in this research, a novel method is introduced for real-time detection of different types of suspended particles based on ultraviolet-infrared (*UV-IR*) dual resonance spectroscopy[21].

1.3.SI. Double resonance spectroscopy

Double resonance spectroscopy is defined as the use of two resonant one-photon interactions in a single molecule to probe molecular structure and relaxation properties [22]. There are several types of double resonance spectroscopy including IR-UV depletion spectroscopy, IR-UV gain spectroscopy, IR-UV hole-burning, UV-UV hole-burning [23]. The infrared–ultraviolet (IR–UV) double resonance spectroscopy has also proven to be a powerful tool for measurement of conformation-selective vibrational spectra of polyatomic molecules, ions, and their clusters. This technique is based on the change of the vibrational population of the molecule by an IR laser pulse with subsequent detection of this change by a UV laser pulse radiation [24].

2.SI. Experimental

2.1.SI. Sample Introduction system

Whole components of the sample introduction have been shown in Schem. 1.SP.

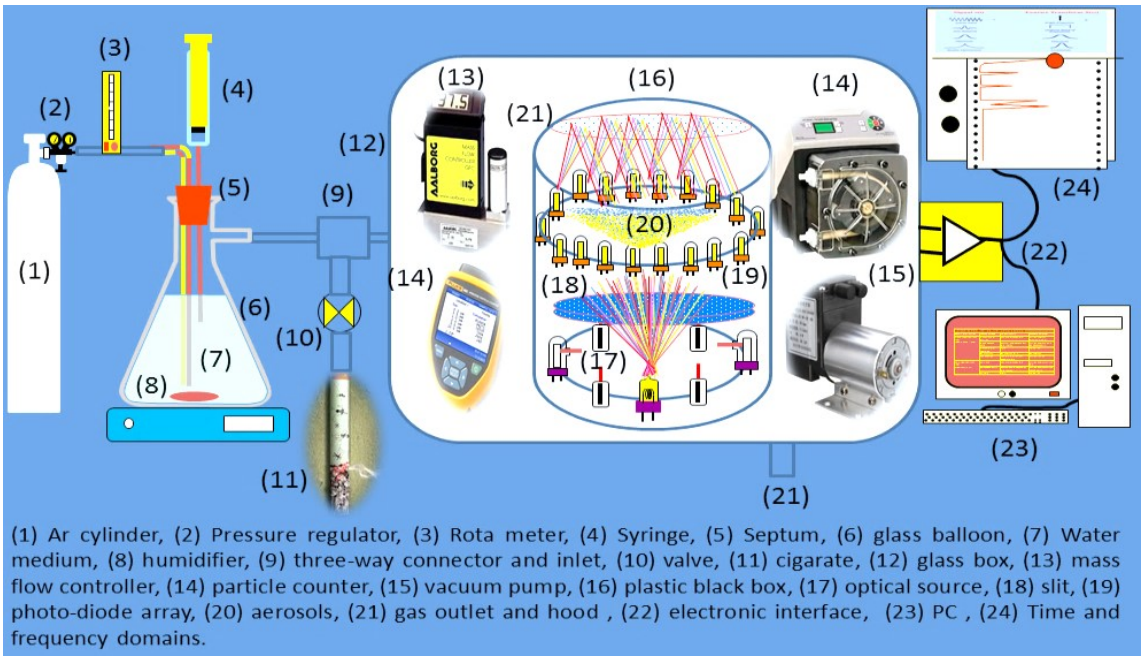

Schem. 1.SP. Schematic of the sample introduction system in the fabricated UV-IR resonance spectrometer for aerosol detection and determination.

2.2.SI. Calibration of the aerosol-based detection system

Due to dependency of the wavelength of the optical sources to the electrical bandwidth as well as the electrical frequency of the digital pulses, applied to each light source, they should be calibrated before any use:

-Experimentally, during estimation of the effective parameters for automatic controlling through the Visual Basic 6 (VB_6) software via following the light frequency bias using a reference (*Commercial*) ultraviolet-visible (*UV-Vis*) spectrophotometer (*LAMBDA 265*). This experiment was achieved in the SA-Iran Center (Shiraz, Iran, optical center, Calibration unit). This experiment was also achieved for controlling the light intensity (sensitivity) via setting the electronically pulse amplitude through the software.

-*Software*, during self-calibration using polystyrene fiber (powder) spray (Hangzhou Hanbang Chemical Fiber Co., Ltd.) as the reference material for calibration of the middle-IR regions

through the software. About the UV-Vis. region, the calibration process was achieved based on the Plasmonic resonance peak of nanoparticles such as gold and silver during reduction of H_2AuO_4 standard solution (0.01 mol L^{-1}, Sigma-Aldrich Company) and $AgNO_3$ (1.0 mmol L^{-1}, Merck Company) using tartaric and tannic acid (0.01 mol l^{-1}, respectively, Merck Company), analog with sizing using transmission electron microscopic imaging according to reported references [25,26].

2.3.SI. Estimation of the fingerprint frequencies

An important characteristic of the written software is its capability for estimation of the fingerprint regions for each spectrum based on measuring the peak area/height of each spectrum at a fixed wavelength region via pixel counting. This capability not only was suitable for identification (qualitative analysis) of any sample, but also adopted for quantitative determination of aerosols as well as counting the aerosol [27].

3.SI. Results and discussion

3.1.SI. Reliability of the detection system

3.1.1.SI. Plasmatic resonance of Ag nanoparticles

Comparison between the plasmatic resonance of the UV-Vis analysis of Ag nanoparticles-containing suspension and that analyzed by reference and commensal UV-Vis. spectrometer (Figure 1.SP) exhibits the reliability of the designed detection system.

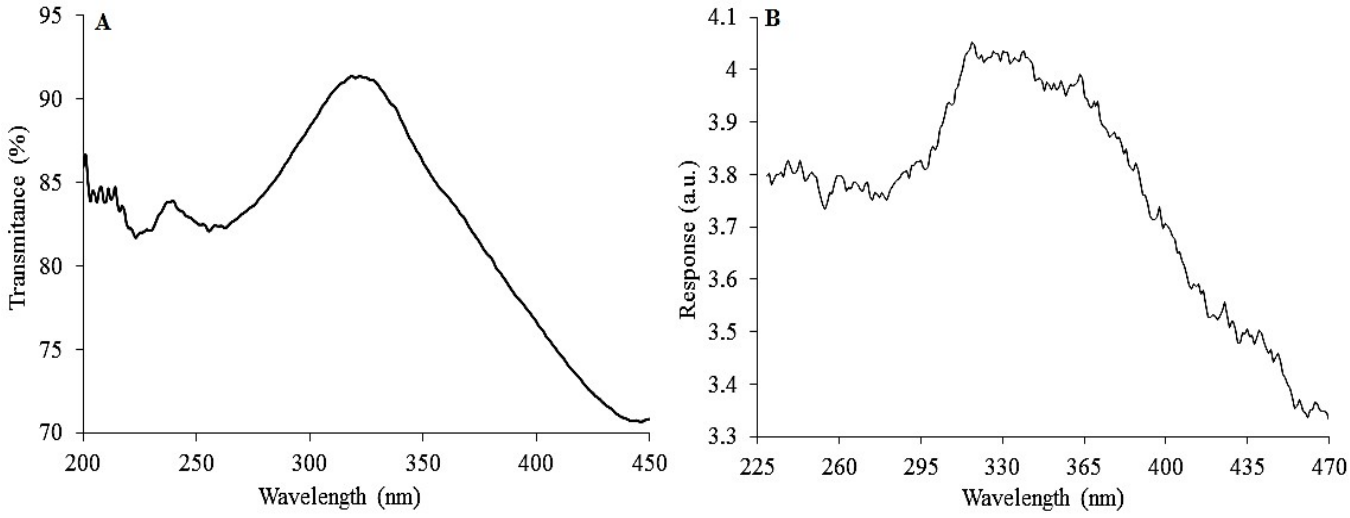

Figure 1.SP. UV-Vis. spectra of Ag nanoparticles using A) standard UV-Vis. spectrometry and B) the fabricated detection system.

The UV-Vis spectra related different types of aerosol such as SiO_2, water, soot and different types of cigarette smog with a constant aerosol population as large as 200 ± 5 were prepared inside argon (*Ar*) as dilution solution. Under similar condition, the ultra violet-visible (*UV-Vis*) spectra of the aerosols using scanning the optical waves with scan rate of 10 ± 1 nm min^{-1} have been shown in Figure 2.SP.

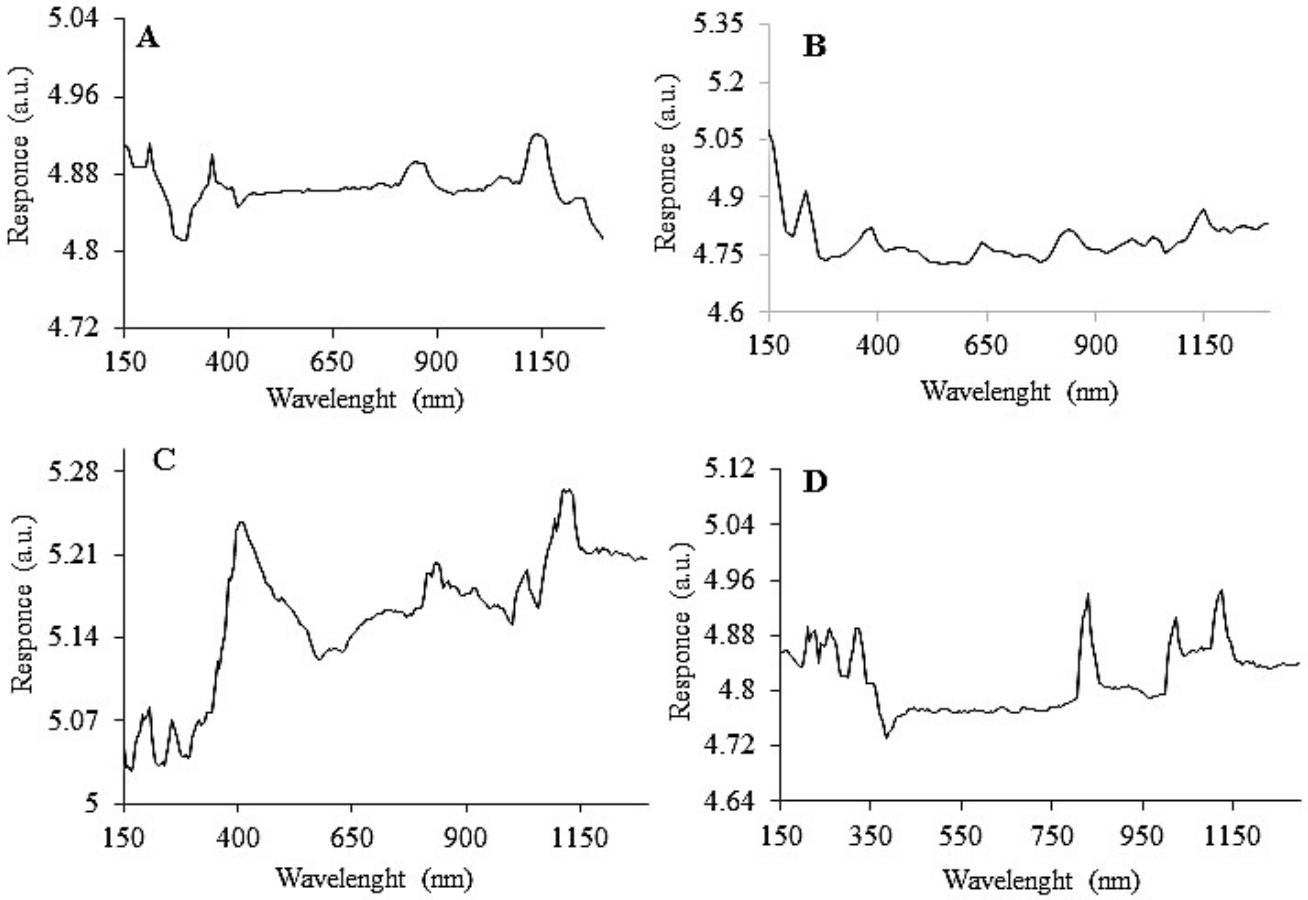

Figure 2.SP. UV-Vis. spectra of different types of water aerosols containing A) $(NH_4)_2SO_4$, B) SiO_2, C) NaCl and D) $NaNO_2$ with 1.0 ± 0.1 mmolar concentrations at a fixed average aerosol size distribution as large as 200 ± 5 at different wavelength regions at scan rate 10 nm min^{-1}.

3.1.2.SI. Middle infrared analysis of polycarbonate powders

In this study, the reliability as well as the accuracy of the obtained peaks was also evaluated in detail via analysis of a polycarbonate powders as reference material [28] for testing the spectrometric systems at the middle-IR region (Figure 3.SP). As shown, maximum similarity was observed during comparing between the UV pulse beam at the λ_{max} and the middle-IR between 400-4000 cm^{-1} and the IR spectrum reported in Ref .[29].

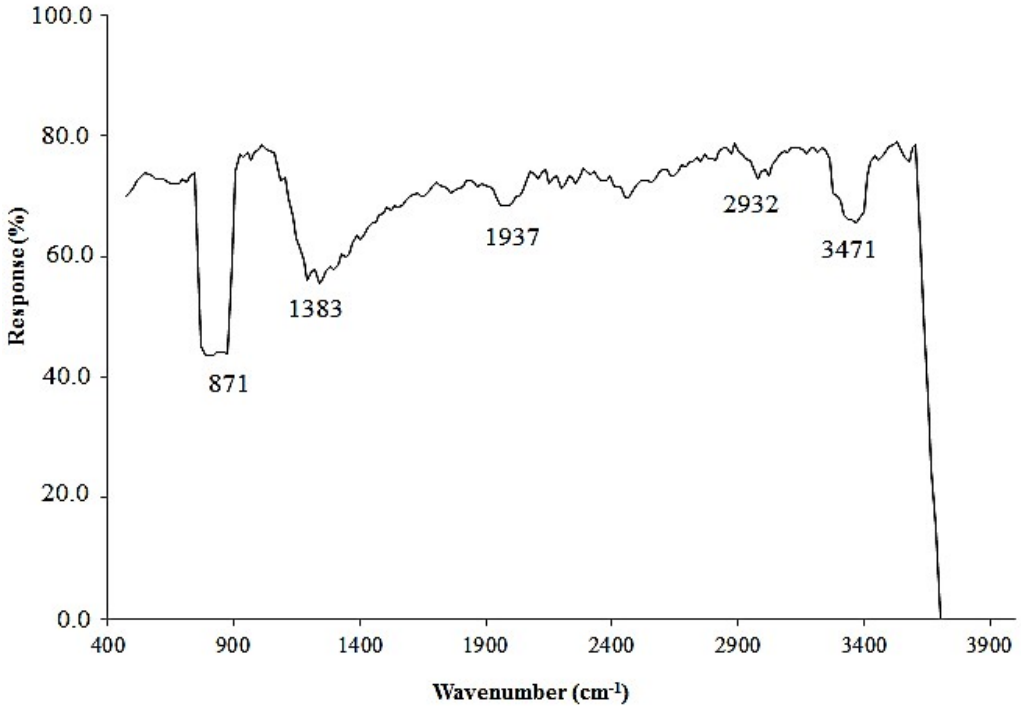

Figure 2.SP. Middle-IR spectrum of polystyrene fiber aerosols (population: 200 ± 5, n=3) during combination of UV with λ_{max} = 260 nm pulse light and during scanning the middle-IR region between 400-4000 cm^{-1}.

3.2.SI. Fourier transform-assisted Ultraviolet-infrared dual resonance spectroscopy

To enhance the sensitivity of the detection system, it was decided to adopt the "Discrete Fast Fourier Transform" (DFFT) algorithm according to the recommended procedure. The free induced decays (FIDs) as well as the spectra in both the presence and absence of the UV pulse light have been shown in Figure 3.A.SP. The sequence decays were also clearly shown in the FID diagram in Figure 3.B.SP. As exhibited, significant enhancement was observed in the sensitivity when coupling the spectroscopic system with the DFFT algorithm.

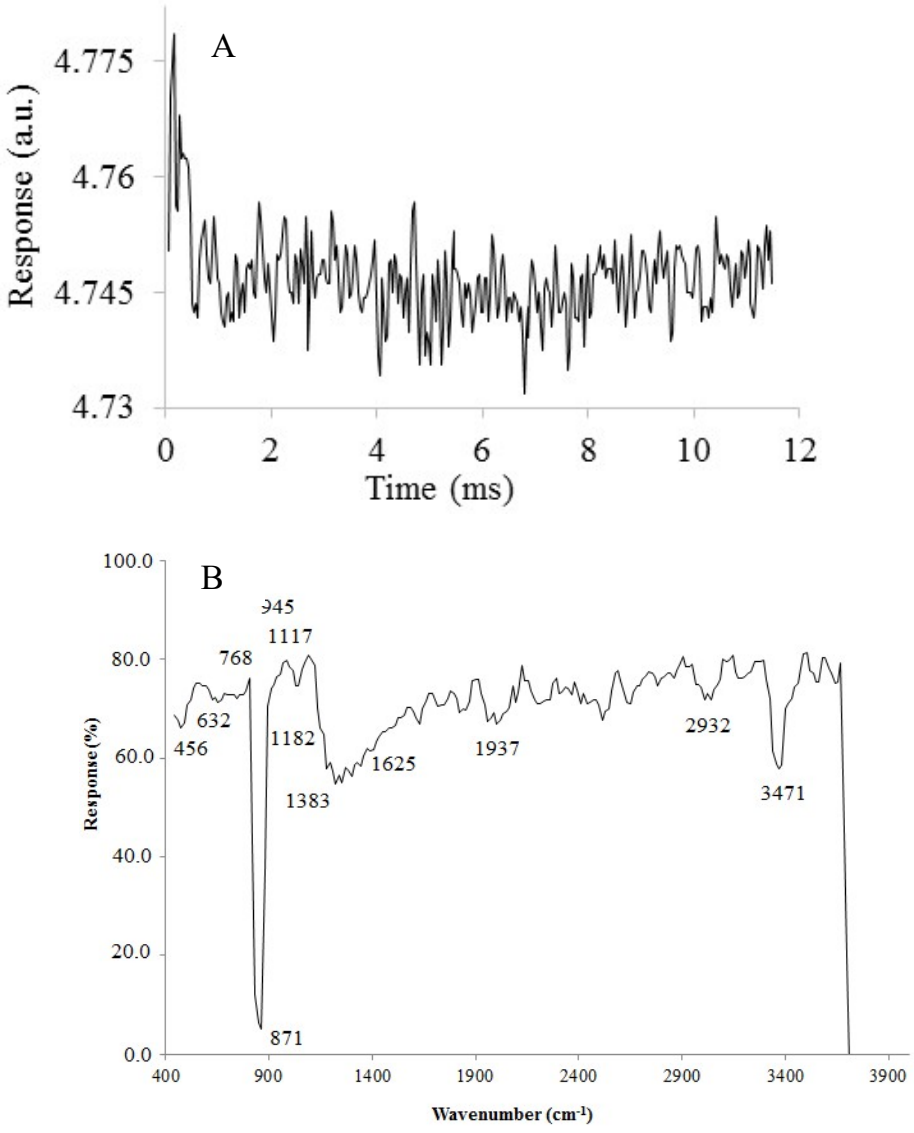

Figure 3.SP. A) FID diagram showing the sequential decay process, B) middle-IR spectrum of polystyrene fiber aerosols with population of 200 ± 5 during combination with UV with λ_{max} = 250-270 nm pulse light and all the wave number regions at the 400-4000 cm^{-1}, IR scan rate: 10 ± 1 cm^{-1} min^{-1}.

3.3.SI. FID averaging based on the switching property of the UV radiation

The sensitivity of this detection system was further enhanced via promotion of the number (no.) of FIDs during their averaging process, resulted in having enhancement in the signal-to-noise

ratio up to at least 30 numbers with eth order of $n^{1/2}$, in which n is considered as the number of averaging (replicate analyses). The effect of a visible pulse beam at 500-520 nm was evaluated as shown in Figure 4.A.SP.

These properties were related to the dual role of the UV-Vis light that, from one hand, had resonance with the IR radiation; and from the other side, its significant sensitivity was considered as a switching time for recognition of the starting time of the FID, for having reproducible segmented analysis as well as possibility to enhancing the signal-to-noise ratio by the averaging process. It also should be noted that, in this experiment, the effect of the DFFT algorithm was evaluated via simultaneous radiation of the UV pulse and a combination of IR beams a certain IR region. At this condition, partially, all the active sites, having spectroscopic probability for having different optical interaction with the lights were almost evaluated. But, the intrinsic Brownian and random motions of the aerosols especially during their circulation by the adopted peristaltic pump caused to have segmented multiple analyses without any need to shutting down the light sources, prior the data sampling the FIDs.

3.4.SI. Dual resonance between UV and far/near IR

To further study about this resonance behavior, dual effect of UV light was evaluated during following the spectrum as different IR modes such as Far-IR and near IR modes via analysis of aerosols under similar conditions (Figures 4.B.SP and 4.C.SP).

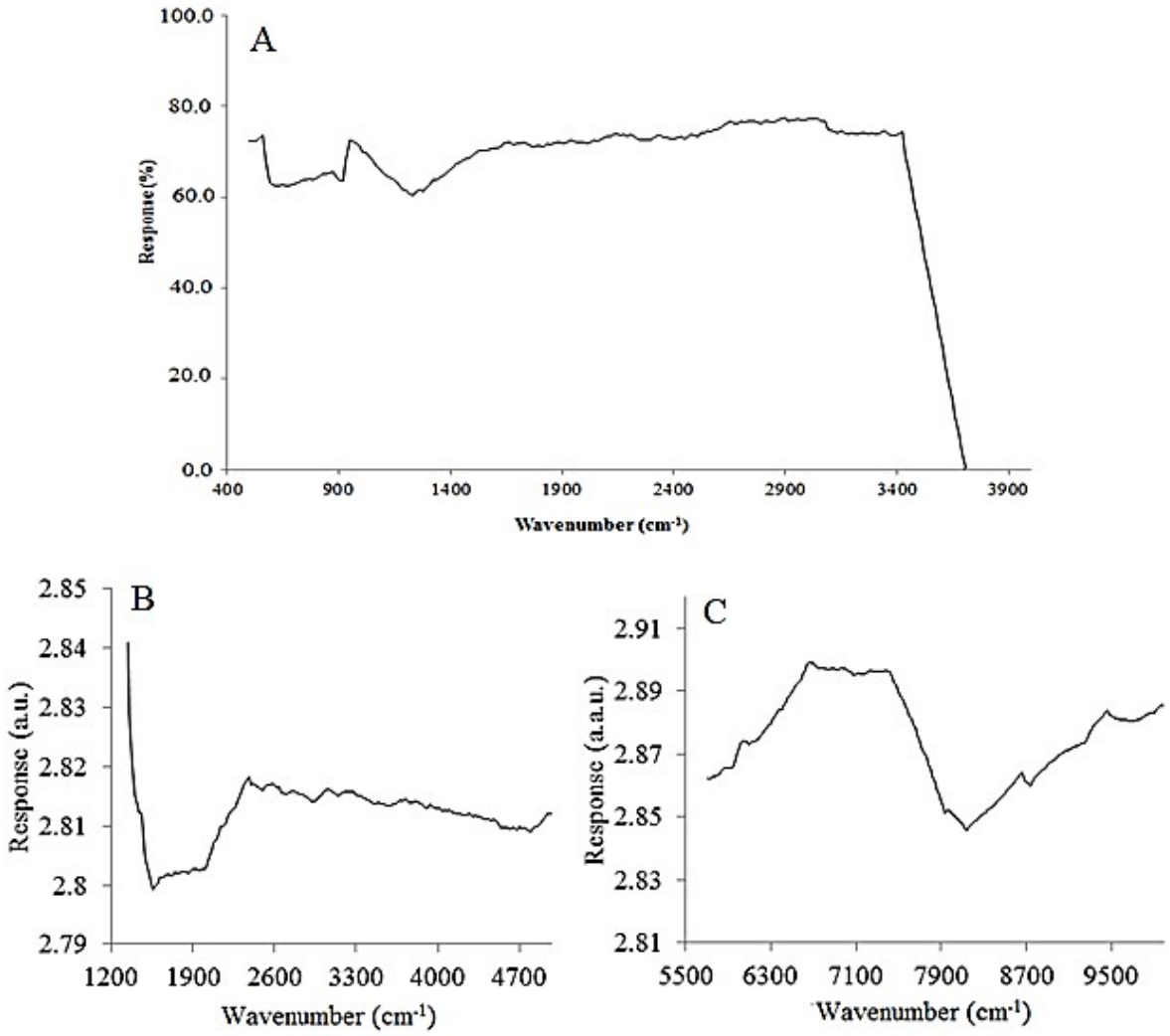

Figure 4.SP. A) Middle-IR spectra of polystyrene powder during combination of the visible with λ_{max} = 500-520 nm pulse light and all the wavelengths regions at the 400-4000 cm^{-1}. No. of FIDs= 30, B) Far- and C) Near- IR spectra of different aerosols during combination of UV with λ_{max} = 250-270 nm and Far-, and near- IR regions. IR scan rate: 10 ± 1 cm^{-1} min^{-1}.

As shown, the number of peaks detected for the spectra at the middle-IR region (Figure 4.SP) was not comparable with those evaluated for the Far- and near- IR modes (Figure 5.SP). Consequently, the spectra at the middle-IR region were selected for detection, recognition and speciation of different types of aerosols. Middle-IR spectra of different kinds of aerosols were

shown in Figure 5.SP. As exhibited, significant differences were observed in the peaks frequencies during analysis of different kinds of areoles that revealed the importance of the interpretation of these spectra for the detection and speciation of aerosols based on evaluation of some peak frequency as "*Fingerprint*" for each aerosol. In this experiment, the fingerprint frequencies were reported based on the evaluation of distinct peaks, belonged to each type of aerosols. As shown (Figure 5.SP), some noticeable differences were observed in the fingerprint frequencies that pointed to the possibility of this method for its use in the detection and determination purposes.

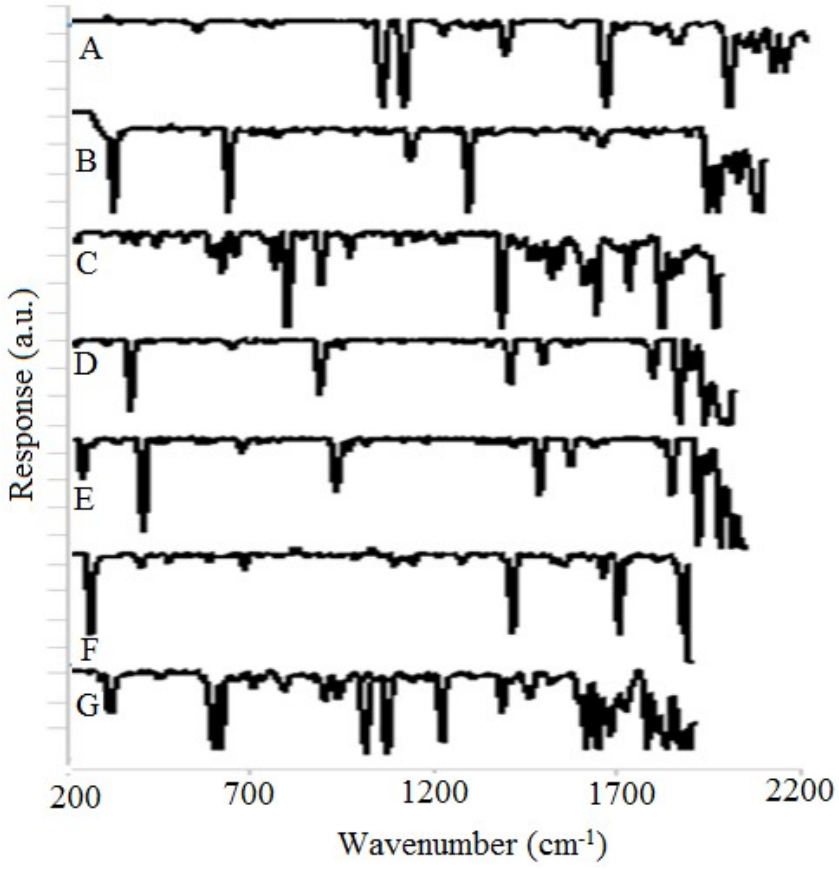

Figure 5.SP. Middle-IR spectra of water aerosols containing different type of aerosols including A) Winston cigarette, B) Marlboro cigarette, C) Espand, D) water, E) perfume, F) paper soot and G) poppy during combination of the UV-Vis. pulse beam at the λ_{max} and all the mid-IR

wavelengths between 400-4000 cm^{-1} region. No. of FIDs= 30. Aerosol population: 200 ± 5, IR scan rate: 10 ± 1 cm^{-1} min^{-1}.

3.5.SI. Figures of merit

3.5.1.SI. Qualitative analysis: Type of Aerosols

In Table 1.SP, list of fingerprint peaks related to the different tested kinds of cigarettes by this detection system have been shown.

Table 1.SP. Fingerprint regions during analysis of various types of the aerosols.

Type of aerosols	**Finger print (cm^{-1} ± 1 , n=3)**	**Sharpest peak position (cm^{-1}, ± 1, n=3)**
Winston cigarette	1056, 1082, 1410, 1621, 1857	1056, 1082
Montana cigarette	372, 681, 1085, 1312, 1827, 2135	1312
Marlboro cigarette	375, 684, 1105, 1316, 2143	1316
Pall mall cigarette	371, 694, 1072, 1321, 2187	1321
Quantum cigarette	362, 705, 1056, 1327, 2181	1327
Williams cigarette	361, 711, 1041, 1342, 1821, 2182	1342
Bahman cigarette	357, 705, 1029, 1335, 1812, 2188	1335
Camel cigarette	351, 716, 1031, 1345, 1837, 2159	1345

Note: *The finger print frequencies were measured based on the conformity of the frequencies during at least three replicate analyses of singe or mixture of aerosol samples.*

3.5.2.SI. Quantitative aspect of the detection system for particle counting purposes

To investigate the quantitative aspect, effect of different probes such as the summation of and peak areas and heights at a certain wavenumber region such as 200-2100 cm^{-1} were evaluated in detail as shown in Figure 6.SP.

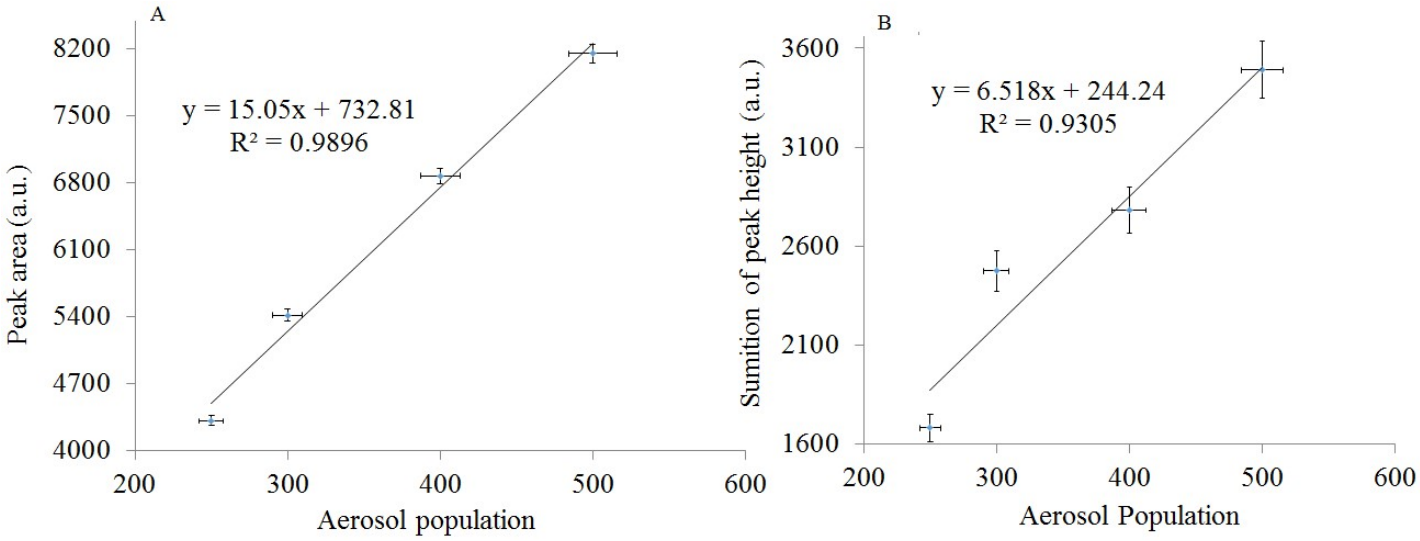

Figure 6.SP. Effect of peak area and peak height on the lineally and reproducibility during analysis water aerosol with differ population ranged between 200-600 particles per m^3. The responses were the summation of peak heights and peak area at 200-2100 cm^{-1} wavenumber region. Data are the average of three replicate analyses, error bars: ±standard deviation.

3.6.SI. Real sample analysis

The reliability of this method was adopted for the total particle counting of different kinds of areoles (Table 2.SI).

Table 2.SI. Estimation of areoles particle counts during analysis of different kinds of aerosols.

Aerosol' s type	Particle counts		Relative error percentage (%, n=3)
	[1]Introduced methods	[2]Ref. probe	
Bahman cigarette	215 ± 4	200 ± 5	+7.50
Paper soot	241 ± 6	25 0±5	-3.60
Perfume	287 ± 7	300 ± 5	-4.33
SiO_2	372 ± 4	350 ±5	+6.28
Poppy	437 ± 7	400 ± 5	+9.25
Water	483 ± 6	500 ± 5	-3.40
Espand	631 ± 8	600 ± 5	+5.17

[1]The data are average of three replicate analyses. ±: Standard deviation. [2] The Ref. probe was sued for simultaneous and real-time count the introduced aerosol samples.

References

(1) Pramod Kulkarni, Paul A. Baron, K. W. *Aerosol Measurement: Principles, Techniques, and Applications*; 2011.

(2) Kulkarni, P.; Baron, P. A.; Willeke, K. Introduction to Aerosol Characterization. *Aerosol Meas. Princ. Tech. Appl.* **2011**, *3*.

(3) Ian Colbeck, M. L. *Aerosol Science: Technology and Applications*; John Wiley & Sons, 2014.

(4) Lazaridis, I. C. M. *Aerosol Science: Technology and Applications*; Colbeck, I., Lazaridis, M., Eds.; John Wiley & Sons, Ltd: Chichester, UK, 2013. https://doi.org/10.1002/9781118682555.

(5) Vincent, J. H. *Aerosol Sampling: Science, Standards, Instrumentation and Applications*; John Wiley & Sons, 2007.

(6) Colbeck, I.; Lazaridis, M. *Aerosol Science*; Wiley Online Library, 2014.

(7) Levin, Zev, Cotton, W. R. *Aerosol Pollution Impact on Precipitation*; Springer, 2009.

(8) Theisinger, S. M.; Smidt, O. de. Bioaerosols in the Food and Beverage Industry. In *Ideas and Applications Toward Sample Preparation for Food and Beverage Analysis*; InTech, 2017. https://doi.org/10.5772/intechopen.69978.

(9) Eneh, O. C. Biological Weapons-Agents for Life and Environmental Destruction. *Res. J. Environ. Toxicol.* **2012**, *6* (3), 65.

(10) D.S., E. *Aerosol Science and Technology: History and Reviews*; 2011.

(11) Pray, S. L. K. and A. A. F. M. and L. A. *Biological Threats and Terrorism*; National Academies Press: Washington, D.C., 2002. https://doi.org/10.17226/10290.

(12) Raymond A. Zilinskas, E. *Biological Warfare: Modern Offense and Defense*; 1999.

(13) Pan, Y.-L. Detection and Characterization of Biological and Other Organic-Carbon Aerosol Particles in Atmosphere Using Fluorescence. *J. Quant. Spectrosc. Radiat. Transf.* **2015**, *150*, 12–35. https://doi.org/10.1016/j.jqsrt.2014.06.007.

(14) Zarzana, K. J.; Cappa, C. D.; Tolbert, M. A. Sensitivity of Aerosol Refractive Index Retrievals Using Optical Spectroscopy. *Aerosol Sci. Technol.* **2014**, *48* (11), 1133–1144. https://doi.org/10.1080/02786826.2014.963498.

(15) Després, V.; Huffman, J. A.; Burrows, S. M.; Hoose, C.; Safatov, A.; Buryak, G.; Fröhlich-Nowoisky, J.; Elbert, W.; Andreae, M.; Pöschl, U. Primary Biological Aerosol Particles in the Atmosphere: A Review. *Tellus B Chem. Phys. Meteorol.* **2012**, *64* (1), 15598.

(16) K. L. Aplin and R. G. Harrison. The Interaction between Air Ions and Aerosol Particles in the Atmosphere,. *Inst. Phys. Conf. Ser* **2012**, *163*, 411–414.

(17) Ohta, S.; Okita, T. A Chemical Characterization of Atmospheric Aerosol in Sapporo. *Atmos. Environ. Part A. Gen. Top.* **1990**, *24* (4), 815–822.

(18) Bokoye, A. I.; Royer, A.; O'Neil, N. T.; Cliche, P.; Fedosejevs, G.; Teillet, P. M.; McArthur, L. J. B. Characterization of Atmospheric Aerosols across Canada from a Ground-based Sunphotometer Network: AEROCAN. *Atmosphere-Ocean* **2001**, *39* (4), 429–456. https://doi.org/10.1080/07055900.2001.9649687.

(19) Baron, P. A.; Willeke, K. Aerosol Fundamentals. *Aerosol Meas. Princ. Tech. Appl.* **2001**, *2*.

(20) Lack, D. A.; Lovejoy, E. R.; Baynard, T.; Pettersson, A.; Ravishankara, A. R. Aerosol Absorption Measurement Using Photoacoustic Spectroscopy: Sensitivity, Calibration, and Uncertainty Developments. *Aerosol Sci. Technol.* **2006**, *40* (9), 697–708. https://doi.org/10.1080/02786820600803917.

(21) Ault, A. P.; Axson, J. L. Atmospheric Aerosol Chemistry: Spectroscopic and Microscopic Advances. *Anal. Chem.* **2017**, *89* (1), 430–452. https://doi.org/10.1021/acs.analchem.6b04670.

(22) H. Kurreck, B. Kirste, W. Lubitz.Sutcliffe, L. H. Electron Nuclear Double Resonance Spectroscopy of Radicals in Solution. Application to Organic and Biological Chemistry. *Magn. Reson. Chem.* **1989**, *27* (4), 407–407. https://doi.org/10.1002/mrc.1260270421.

(23) Nir, E.; Janzen, C.; Imhof, P.; Kleinermanns, K.; de Vries, M. S. Pairing of the

Nucleobase Guanine Studied by IR–UV Double-Resonance Spectroscopy and Ab Initio Calculations. *Phys. Chem. Chem. Phys.* **2002**, *4* (5), 740–750. https://doi.org/10.1039/b110360c.

(24) Plützer, C.; Nir, E.; de Vries, M. S.; Kleinermanns, K. IR–UV Double-Resonance Spectroscopy of the Nucleobase Adenine. *Phys. Chem. Chem. Phys.* **2001**, *3* (24), 5466–5469. https://doi.org/10.1039/b107997b.

(25) Paredes, A. M. MICROSCOPY | Transmission Electron Microscopy. In *Encyclopedia of Food Microbiology*; Elsevier, 2014; pp 711–720. https://doi.org/10.1016/B978-0-12-384730-0.00216-0.

(26) Williams, D. B. Electron Microscopy: Transmission. In *Encyclopedia of Materials: Science and Technology*; Elsevier, 2001; pp 2577–2584. https://doi.org/10.1016/B0-08-043152-6/00466-6.

(27) Feng, J.; Zhou, J.; Jain, A. K. Orientation Field Estimation for Latent Fingerprint Enhancement. *IEEE Trans. Pattern Anal. Mach. Intell.* **2012**, *35* (4), 925–940.

(28) Brunelle, D. J.; Smith, W. E. Polycarbonate Transesterification Process. Google Patents August 1980.

(29) Hurley, M. D.; Wallington, T. J.; Buchanan, G. A.; Gohar, L. K.; Marston, G.; Shine, K. P. IR Spectrum and Radiative Forcing of CF4 Revisited. *J. Geophys. Res. Atmos.* **2005**, *110* (D2).